ISTITUTO NAZIONALE DI FISICA NUCLEARE

Sezione di Genova

INFN/TC-86/1
27 Gennaio 1986

Revised version
25 Marzo 1986

F. Levrero, R. Parodi and S. Terreni:

POLARIZED HYDROGEN BEAM TARGET

Servizio Documentazione
dei Laboratori Nazionali di Frascati

INFN - ISTITUTO NAZIONALE DI FISICA NUCLEARE
Sezione di Genova

INFN/TC-86/1
27 Gennaio 1986

POLARIZED HYDROGEN BEAM TARGET

F. LEVRERO, R. PARODI e S. TERRENI
Istituto Nazionale di Fisica Nucleare e Dipartimento di Fisica dell'Università

1. - INTRODUCTION

A polarized hydrogen beam target to be used in high energy particle accelerators is presented

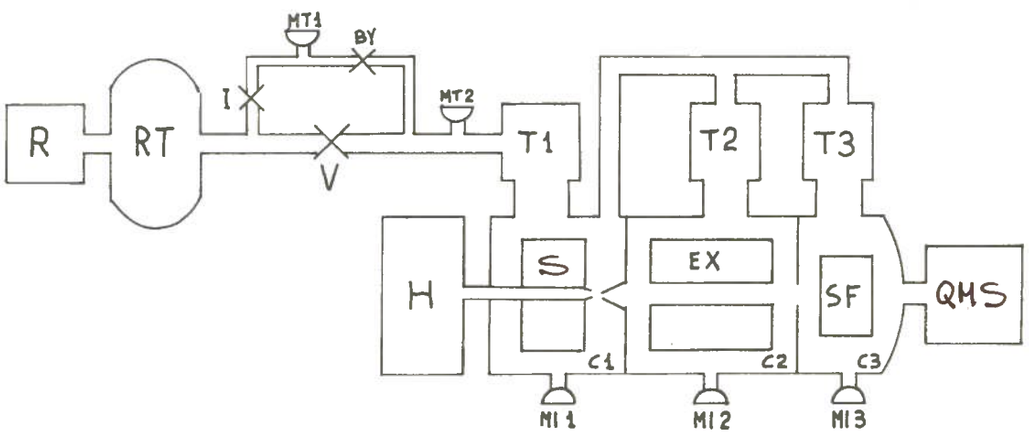

Fig. 1 - The whole apparatus.

A schematic view of the apparatus is shown in Fig.1: the atomic hydrogen beam produced by a microwave discharge in the source S passes through the hexapole magnet EX which focuses in the interaction region the atoms with the electronic spin antiparallel to the local magnetic field.

The spin-flip stage SF destroys the electron spin polarization and produces a beam with polarized nuclear spin (1).

The source, hexapole and spin-flip chambers C1, C2, C3 are evacuated by turbomolecular pumps LEYBOLD-HERAEUS TURBOVAC 1000 (T_1 and T_2 in Fig.1) and TURBOVAC 360 (T_3 in Fig.1) with conventional rough pumps LEYBOLD-HERAEUS RUVAC WA 251 and TRIVAC D60A (RT and R in Fig.1).

In this note we present the first two stages of the apparatus: the atomic hydrogen source, described in section 1, and the hexapolar magnet focusing system, described in section 2, which were tested by monitoring the beam density with the quadrupolar mass spectrometer QMS. The experimental results are reported in section 3.

2. - ATOMIC HYDROGEN SOURCE

Fig.2 shows a schematic drawing of the beam production system.

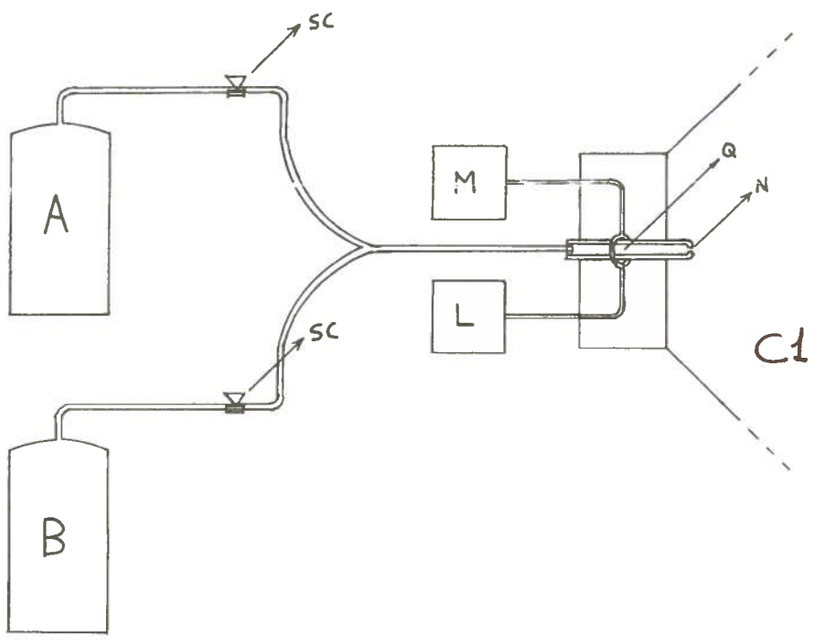

Fig. 2 - The beam production system.

The A and B bottles contain respectively hydrogen and oxygen. The oxygen has an accessory function: it is mixed in amount of few percent to Hydrogen in order to improve the dissociation efficiency.

The hydrogen-oxygen mixture is supplied to the quartz tube Q which is ended by the nozzle N. The tipical nozzle throat diameter is .5 mm. The quartz tube is located in a high impedence region of a transmission line which acts as an electric field transformer (2).

The RF power for the H_2 dissociation is supplied by the magnetron M. L is a RF load (NARDA 50Ω, 175 W).

The pressure upstream the capillary SC is set at values ranging from 1 to 4 abs. atm. The capillary SC has impedence much higher than the nozzle in order to set the pressure inside the quartz tube at values of a few mbar.

The H_2 throughput is measured by reading the pressure p_1 in the C_1 chamber as (3)

$$\Phi H_2 = 1.83 \times p_1 S_1$$

where S_1 = 1000 l/sec is the pumping speed in C_1 and the numerical factor accounts for the ionization efficiency of H_2.

The O_2 gas supply line is similar to H_2 line but the impedance of its capillary is a factor 100 higher.

The O_2/H_2 pressure ratio in the quartz tube is obtained from the measurement of the ratio $\Phi O_2/\Phi H_2$ taking into account the different thermal velocities of the two species.

The magnetron M (EMS MICROTRON 200) supplies to the broad band field transformer a maximum RF power of 200 W on an output impedance of 50Ω at a frequency of 2450 HHz.

The transmission line is ended by a 50Ω RF load L which match the impedance of the field transformer at the output inpedance of the magnetron avoiding microwave power reflection.

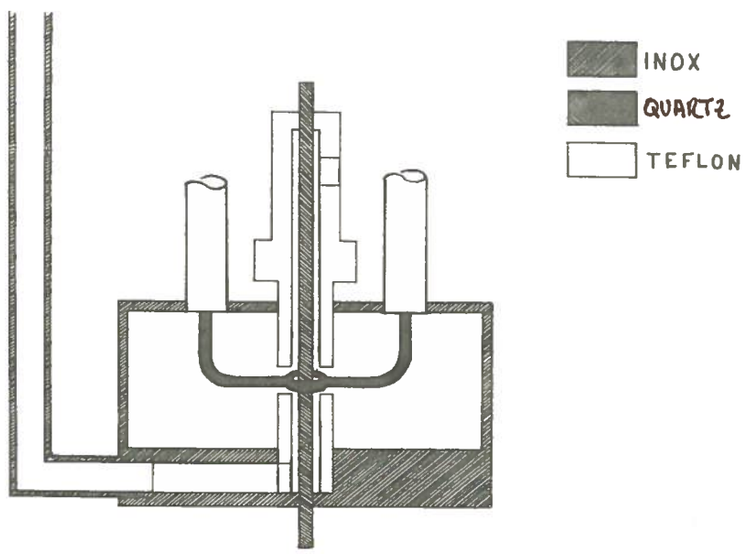

Fig. 3 - The atomic hydrogen beam source.

Fig. 3 shows a sketch of the source: the quartz tube crosses the microwave transmission line in the high impedence region where the electric field is high enough to mantain the discharge in a stationary regime but not enough in order to start the discharge which has to be started by means of a H.F. sparck produced by a Teslacoil.

The discharge can be substained at pressure values ranging from about .1 torr to 20 torr. Only about the 10% of the power adsorbed by the discharge is carried by the dissociated beam, while the remaining 90% is transfered to the quartz tube walles by surface and volume H recombination.

The discharge tube is cooled by a forced flow of pressurized air or cold nitrogen vapours as shown in Fig.3.

3. - FOCALIZATION SYSTEM

The magnetic hexapole located in the C_2 chamber focuses in the interaction region the atoms with spin antiparallel to the local magnetic field.

Table 1 reports the main hexapole constructive features.

external cylinder dimensions	190 x 100 mm
expansions dimensions	14 x 78 x 200 mm
number of coil winding	272
winding wire diameter	1.2 mm
coil resistance	2350
expansions field (50V 3A)	7 KGauss

TABLE 1 - Magnetic hexapole construction features

The hexapole acts on the beam atoms as a chromatic lens, focusing in different axial points atoms having different velocities.

The system has been designed in order that atoms having velocities between 2000 m/s and 3500 m/s enter the final collimator.

3.1 - Spin selection

The magnetic field inside the hexapolar magnet has cylindrical symmetry and modulus given by (4)

$$B = B_o \left(\frac{r}{r_o}\right)^2$$

where r_o is the radius of the cylinder tangent to the magnetic expansions and B_o is the magnetic field modulus at this cylinder. Inside the hexapole the H atoms energy levels are splitted according to the hyperfine levels diagram of Fig.4 where the single arrows refer to the electronic spin states ($\uparrow \Rightarrow m_e = + 1/2$) and the arrows with a bar to the nuclear spin states ($\updownarrow \Rightarrow m_N = + 1/2$).

Only $|b\rangle$ and $|d\rangle$ are pure states for every field value, while $|a\rangle$ and $|c\rangle$ are in general mixed states. The mixing parameter Θ in high field approaches zero asymptotically ($\Theta \rightarrow 0$) according to

$$\sin\Theta \quad \frac{a}{2\mu^+ B}$$

where a is the energy gap in zero magnetic field, $\mu^{\pm} = g_e k_e \pm g_N k_N$ (k_e, K_N electronic and nuclear magneton, g_e, g_N electronic and nuclear g-factors) and B the magnetic field.

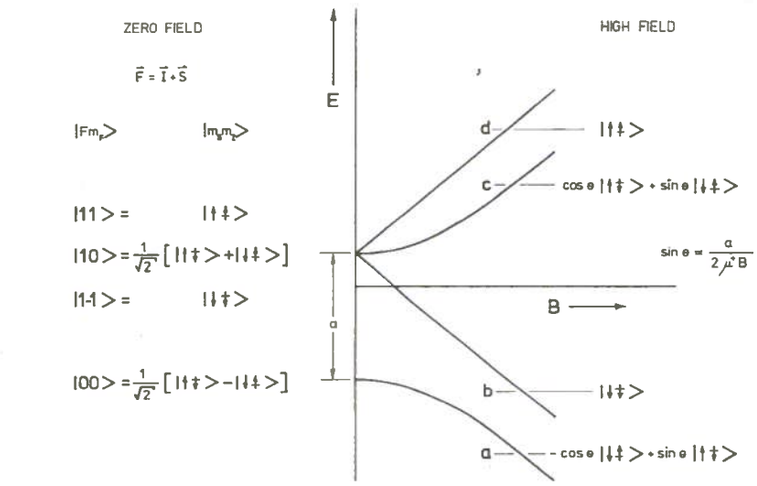

Fig.4 - Hyperfine levels of a hydrogen atom.

The force acting on the atoms in the magnetic field is radial and its modulus is

$$F = 2\mu_e B_o \frac{r}{r_o^2}$$

Atoms lying in the two upper hyperfine levels have positive μ_e, and are focalized. On the contrary atoms lying in the lower levels are defocalized.

So the beam is electronically polarized, except for the small depolarized part present in the mixed state $|c\rangle$.

The magnetic field must be kept at the highest possible value in order to obtain the highest beam polarization. In our apparatus we have choosed a magnetic field strength of .7 Tesla in order to avoid the worsening of the vacuum, due to the coil outgassing, in the C_2 chamber.

3.2 - Velocity selection

In magnetic fields higher than 100 Gauss the H atom motion may be described by means of the adiabatic approximation which assumes the conservation of the magnetic moment along the local direction of the field.

The atomic motion inside the haxapole is the superposition of an axial uniform motion and of a radial motion which, in the adiabatic approximation, is harmonic with frequency

$$\omega = \sqrt{\frac{2\mu_{//} B_o}{r_o^2 m}} \simeq 2 \cdot 10^6 \ s^{-1}$$

where $\mu_{//}$ is the μ component parallel to the local field and m is the H mass.

The typical situation is shown in Fig. 5.

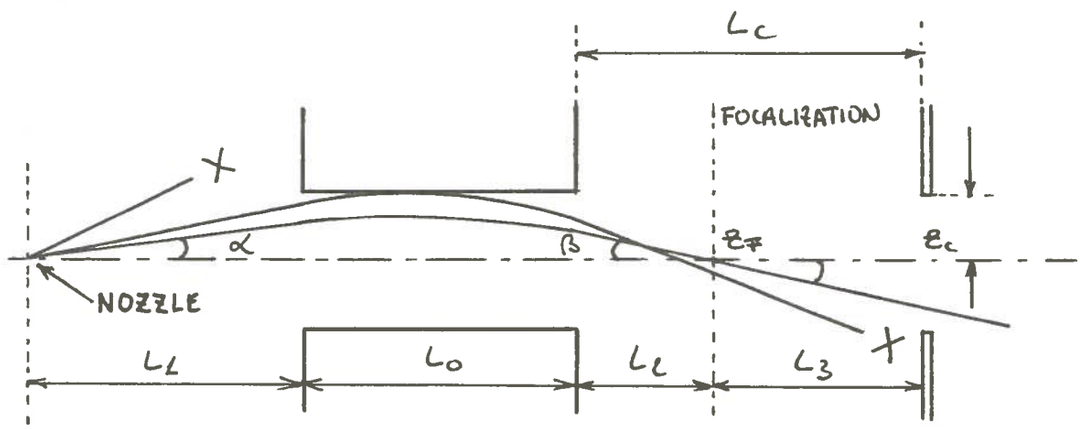

Fig. 5 - Trajectories of atoms in the focalization system.

The detailed calculations of the trajectories was performed by using the transfer matrix method in the paraxial approximation.

The focal point of the magnetic system is given by the solution of the following equation (5):

$$\operatorname{cotg} \frac{\omega}{V} L_o = \frac{\omega}{V} \frac{L_1 L_2 - V^2/\omega^2}{L_1 + L_2}$$

where V is the atom velocity, ω the harmonic radial motion frequency and L_o, L_1, L_2 the distances shown in Fig. 5.

The acceptance Ω of the system i.e. the solid angle, centered on the nozzle, inside which atoms are transmitted is

$$\Omega = \pi \frac{r_o^2 \omega^2}{v^2 + \omega^2 L_1^2}$$

if the final collimator (of radius r_o) does not causes atom losses, and is

$$\Omega = \pi \left[\cos \frac{\omega}{V} L_o - \frac{\omega}{V} L_2 \sin \frac{\omega}{V} L_o \right]^2 \frac{r_o}{d^2}$$

in the opposite case.

We have computed focal distances and acceptance for different velocities and for some values of geometrical parameters L_o, L_1 and L_2.

Typical results are reported in Table 2.

A plot of the system acceptance versus the velocity is shown in Fig. 6 while Fig.7 shows the velocity distribution of the beam entering the final collimator calculated as product of the acceptance by the maxwellian distribution of the atoms emerging from the nozzle.

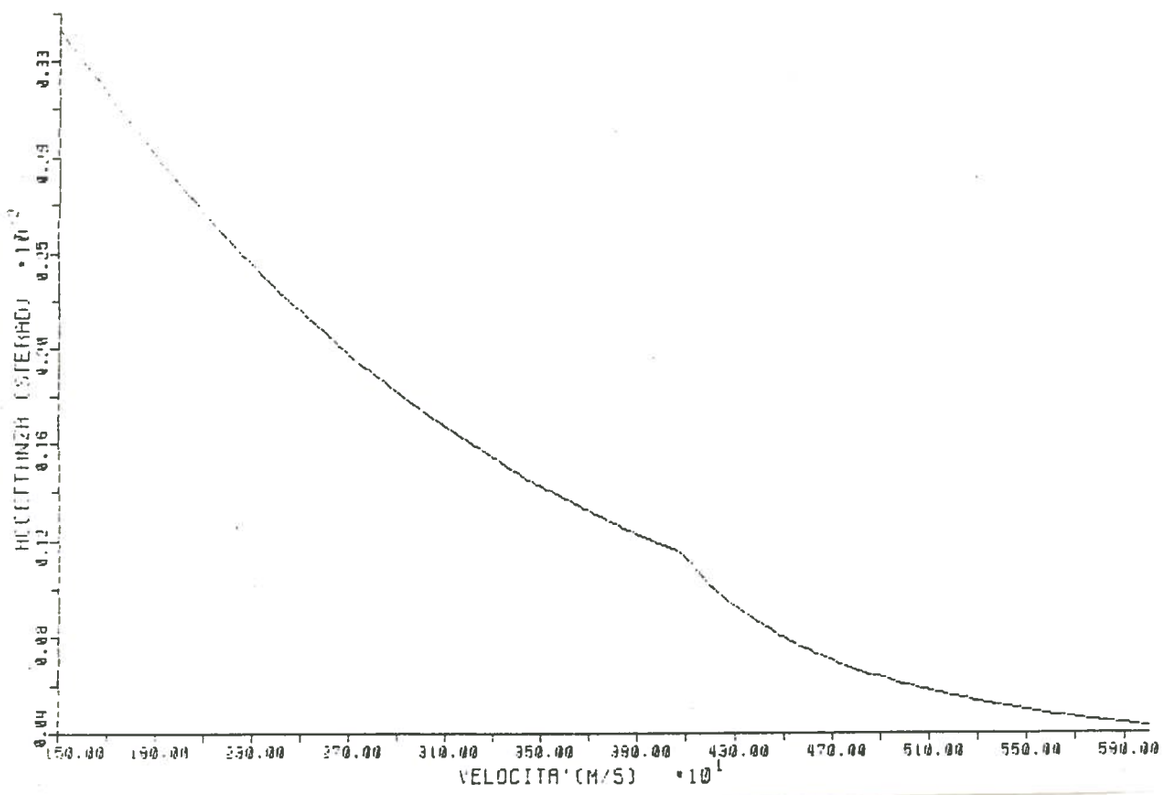

Fig.6 - System acceptance versus velocity

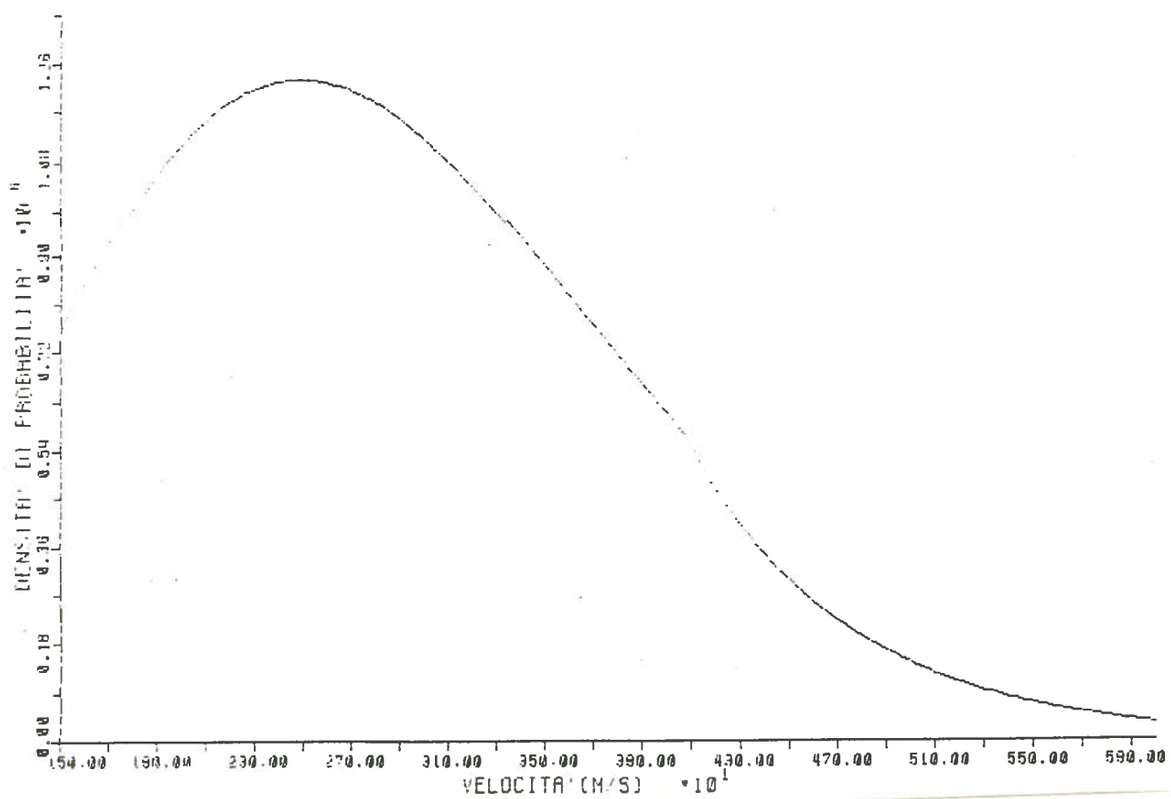

Fig.7 - Velocity distribution of the beam entering the final collimator.

L_1 = 5 cm L_c = 20 cm

VELOCITY (m/s)	FOCAL (cm)	ACCEPT. (sterad)
2284	10	3.8×10^{-3}
2360	12	3.6×10^{-3}
2427	14	3.4×10^{-3}
2487	16	3.3×10^{-3}
2540	18	3.2×10^{-3}
2588	20	3.1×10^{-3}
2670	24	2.9×10^{-3}
2738	28	2.8×10^{-3}
2796	32	2.7×10^{-3}
2845	36	2.6×10^{-3}
2887	40	2.5×10^{-3}
2972	50	2.4×10^{-3}
3036	60	2.3×10^{-3}
3085	70	2.3×10^{-3}
3185	80	2.2×10^{-3}
3184	100	2.1×10^{-3}
3226	120	2.1×10^{-3}
3258	140	2.1×10^{-3}
3283	160	2.0×10^{-3}
3302	180	2.0×10^{-3}
3318	200	2.0×10^{-3}

TABLE 2 - Focalization distances and acceptance for various velocities of atoms.

4. - EXPERIMENTAL RESULTS

We have measured the H and H_2 signals on the mass spectrometer for a few different nozzle diameters and for various pressures in the quartz tube.

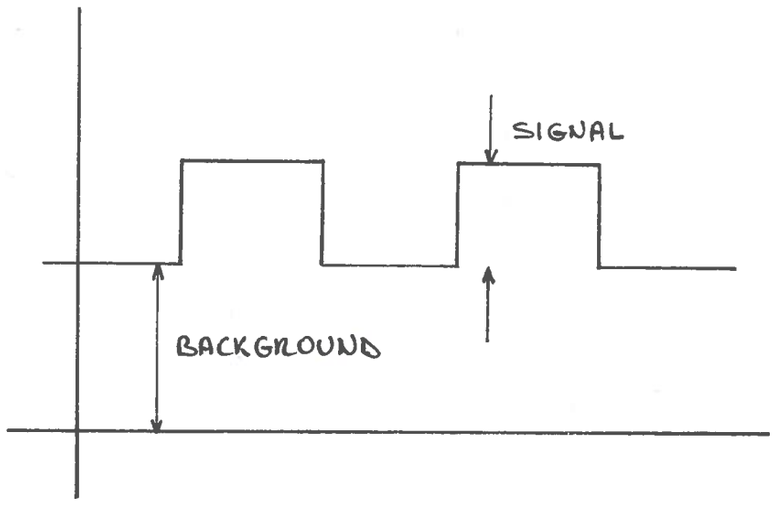

Fig. 8 - The QMS signal

The chopped signal in Fig.8 is due to the beam both for H and H_2.

The background H signal is negligible and is mainly due to the H_2O dissociation in the ionization region of the detector. The H_2 background signal is proportional to the H_2 density in the detector chamber due to the randomization of the H_2 beam molecules and to the recombination followed by randomization of the H beam atoms.

We have calibrated the QMS signal in absolute density accounting that the H_2 background signal corresponds to the density

$$n_{H_2} = \frac{\Delta p}{KT}$$

where Δp is the pressure rise measured in the detector chamber due to the beam. For the chopped H signal the ratio of the ionization efficiency for H and H_2, which is 0.67, was taken into account.

One set of measurements is reported in Table 1.

Nozzle (torr.l/sec)	P (mbar)	n_{H_2} backg ($\frac{\text{molecules}}{cm^3}$)	n_{H_2} beam ($\frac{\text{molecules}}{cm^3}$)	n_H beam HEX OFF ($atoms/cm^3$)	n_H beam HEX ON ($atoms/cm^3$)
0.16	9×10^{-7}	2.2×10^{10}	3.6×10^{9}	3.1×10^{9}	9.4×10^{9}

The dissociation degree of the beam is

$$D = \frac{n_{H_{OFF}}}{n_{H_{OFF}} + 2n_{H_2}} = 30\%$$

The polarization degree of the beam is

$$P = \frac{n_{H_{ON}} + n_{H_2}}{n_{H_{ON}} + 2n_{H_2}} = 79\%$$

5. ACKNOWLEDGEMENTS

We acknowledge the electronic and mechanical workshops of the INFN Genova Section and the CERN mechanical workshop for their skilful work.

6. - REFERENCES

(1) A. Abragam and J.M. Winter, Phys. Rev. Lett. 10, 374(1958).

(2) S. Ramo, J.N. Whinnery and T. Vanduzer "Field and Waves in communicatio electronics", Wiley (1956).

(3) N.F. Ramsey, "Molecular beams", Oxford University Press, New York 1956.

(4) A. Barcellona, M.G. Dondi, V. Lagomarsino, F. Tommasini and U. Valbusa, Proc. IV Simposium on Molecular Beams, Cannes 1973.

(5) F. Levrero, "Realizzazione di un bersaglio di idrogeno gassoso polarizzato per esperimenti di fisica subnucleare", tesi di laurea, Genova.